Proceedings of IDETC'05
2005 ASME International Design Engineering Technical Conferences
Long Beach, USA, September 24-28, 2005

DETC2005-84312

ANALYTICAL INVESTIGATION OF HOPF BIFURCATIONS OCCURRING IN A 1DOF SLIDING-FRICTION OSCILLATOR WITH APPLICATION TO DISC-BRAKE VIBRATIONS

Hartmut Hetzler
Institut für Technische Mechanik
Fakultät für Maschinenbau
Universität Karlsruhe (TH)
Karlsruhe, 76131
Germany
Email: hetzler@itm.uni-karlsruhe.de

Wolfgang Seemann
Institut für Technische Mechanik
Fakultät für Maschinenbau
Universität Karlsruhe (TH)
Karlsruhe, 76131
Germany

Daniel Schwarzer
Institut für Technische Mechanik
Fakultät für Maschinenbau
Universität Karlsruhe (TH)
Karlsruhe, 76131
Germany

ABSTRACT

This article deals with analytical investigations on stability and bifurcations due to declining dry friction characteristics in the sliding domain of a simple disc-brake model, which is commonly referred to as "mass-on-a-belt"-oscillator. Sliding friction is described in the sense of Coulomb as proportional to the normal force, but with a friction coefficient μ_S which depends on the relative velocity. For many common friction models this latter dependence on the relative velocity can be described by exponential functions. For such a characteristic the stability and bifurcation behavior is discussed. It is shown, that the system can undergo a subcritical Hopf-bifurcation from an unstable steady-state fixed point to an unstable limit cycle, which separates the basins of the stable steady-state fixed point and the self sustained stick-slip limit cycle. Therefore, only a local examination of the eigenvalues at the steady-state, as is the classical ansatz when investigating conditions for the onset of friction-induced vibrations, may not give the whole picture, since the stable region around the steady state fixed point may be rather small. The analytical results are verified by numerical simulations. Parameter values are chosen for a model which corresponds to a conventional disc-brake.

INTRODUCTION

A classical model of self-sustained oscillations due to dry friction is the "mass-on-a-belt" model, which has been widely studied over decades (e.g. [1], [2], [3]).

When talking of "stability" concerning this well-known friction oscillator, usually only the linear stability of the steady state is examined by means of eigenvalue analysis, since the destabilization of the steady-state fixed point is one of the possible triggers leading the system to the stick-slip limit cycle. At the same time, all that is happening in between the fixed point and the self-sustained stick-slip cycle is neglected - although dry friction can exhibit nonlinear characteristics. Already in 1958, Kauderer [1] examined the energy balance of the model and predicted the existence of an unstable limit cycle in the sliding domain between the steady-state fixed point and the stick-slip limit cycle for nonlinear friction characteristics.

This article examines the sliding motion of the oscillator including fixed-points, limit-cycles and their stability. After a description of the mechanical model, analytical approximate solutions are derived via an averaging method. In the sequel, these analytical results are used to examine the behavior of a standard model for disc-brake vibration. Finally, the analytical results are checked by numerical simulations and conclusions are given.

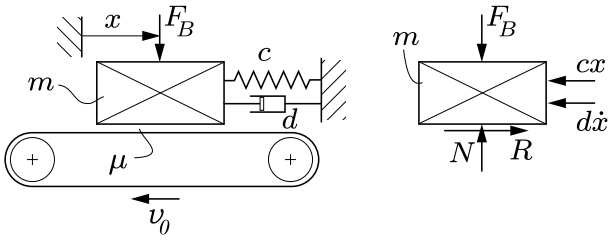

Figure 1. BLOCK-ON-A-BELT-MODELL.

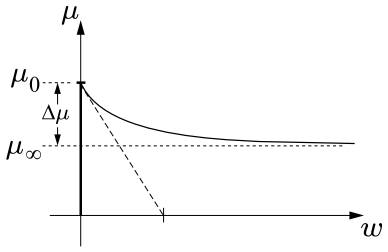

Figure 2. STRIBECK FRICTION WITHOUT VISCOUS INFLUENCES.

MECHANICAL MODEL

Oscillator

The mechanical model comprises a block of mass m, which is pressed onto a moving belt by a normal force F_B, while the belt has the constant speed v_0. The block is connected to the inertial system by a dashpod (damping coefficient d) and a spring (stiffness c). With the relative velocity $w = v_0 - \dot{x}$ between block and belt, the unsteady equation of motion in sense of Filippov reads

$$\ddot{x} + 2D\omega_0\dot{x} + \omega_0^2 x \in R\,, \quad R = \begin{cases} [-\mu_0\frac{N}{m}; +\mu_0\frac{N}{m}] : w = 0 \\ \operatorname{sign}(w)\mu(w)\frac{N}{m} : w \neq 0 \end{cases}, \quad (1)$$

with the dimensionless damping measure $D = \frac{d}{2m\omega_0}$, the eigenfrequency $\omega_0 = \sqrt{\frac{c}{m}}$ of the undamped system and the normal contact force N.

Depending on the relative velocity w the right-hand side either represents sliding friction in the sense of Coulomb ($w \neq 0$) or static friction as a constraint force ($w = 0$), which has to be determined evaluating the kinematic constraint equation describing stiction between belt and block. The latter case is not considered in the following.

Sliding Friction

The sliding friction force is described in the sense of Coulomb as being proportional to the normal contact force N by the coefficient of sliding friction μ. In general, this coefficient depends on a huge variety of parameters. In a first approximation, only the dependence on the relative velocity w between the two tribological partners is considered. Therefore, a Stribeck friction characteristic is chosen, which features a $\mu(w)$ that declines with increasing w. Because only dry friction is considered, there is no increase of μ for higher w, as it would be the case in the presence of viscous effects.

Choosing an exponential description, the coefficient of sliding friction can be written as

$$\mu(w) = \mu_\infty + \Delta\mu\,\mathrm{e}^{-a|w|}, \quad (2)$$

with $\Delta\mu = \mu_0 - \mu_\infty$, the absolute value $|w|$ of the relative velocity and a slope parameter a.

One interesting aspect of the chosen friction curve is that other common characteristics may be derived from it. For example, expanding the exponential function and truncating after the linear term yields

$$\mu^*(w) = \mu_\infty + \frac{\Delta\mu}{1 + a|w|}, \quad (3)$$

which is a widely used friction model [4], [1].

Steady-state and its linear stability

In the following, the focus will be on sliding motion in the vicinity of the steady-state fixed point. Here, $w > 0$ holds for the relative velocity between block and belt and therefore the equation of motion reads

$$\ddot{x} + 2D\omega_0\dot{x} + \omega_0^2 x = \frac{N}{m}\mu(w). \quad (4)$$

Obviously the steady-state is at

$$x_S = \frac{N}{m\omega_0^2}\left(\mu_\infty + \Delta\mu\mathrm{e}^{-av_0}\right). \quad (5)$$

In technical applications, only the linear stability of the steady state is considered to answer the question if self-sustained oscillations arise due to a destabilization of the steady state, or not. For this purpose, the equation of motion is linearized around the steady-state and the linear variational equation for the perturbation $\Delta x = x - x_S$ is derived as follows

$$\Delta\ddot{x} + \underbrace{\left[2D\omega_0 + \frac{N}{m}\Delta\mu\left(-a\mathrm{e}^{-av_0}\right)\right]}_{=\delta}\Delta\dot{x} + \omega_0^2\Delta x = 0. \quad (6)$$

Note that the bracketed term $(-a\mathrm{e}^{-av_0})$ gives the local gradient of the friction characteristic at the steady state $\dot{x} = v_0$. For

positive values of a it always is negative and decreases as a is increased.

The steady state is stable if the system is really damped. This is the case if the extended damping term δ is positive, otherwise the system is unstable. In order to correspond to later formulations, the related condition is written as

$$x_S \text{ lin. stable } \leftrightarrow \quad D\omega_0 - \frac{a}{2}\frac{N}{m}\Delta\mu e^{-av_0} > 0. \tag{7}$$

ANALYTICAL APPROXIMATE SOLUTION OF THE SLIDING MOTION

Amplitude Equation by Averaging

In the following, an approximate solution for the sliding oscillator is sought by applying the first order Method of Averaging, cf. [2]. For this purpose, the coordinate transformation $z = x - x_S$ (i.e. $\dot{z} = \dot{x}, \ldots$) is introduced into the equation of motion (4) such that $z = 0$ corresponds to the steady-state. Rearrangement to the so-called standard form and insertion of the friction characteristic (2) yields

$$\begin{aligned}\ddot{z} + \omega_0^2 z &= -2D\omega_0\dot{z} + \frac{N\Delta\mu}{m}\left(e^{-a(v_0-\dot{z})} - e^{-av_0}\right) \\ &= -2D\omega_0\dot{z} + \frac{N\Delta\mu}{m}e^{-av_0}\left(e^{+a\dot{z}} - 1\right).\end{aligned} \tag{8}$$

Obviously the transcendental function in the bracketed term will cause problems when carrying out the averaging procedure. For this reason, it is made analytic by expansion into an infinite series. Doing this gives

$$\begin{aligned}\ddot{z} + \omega_0^2 z &= -2D\omega_0\dot{z} + \sum_{n=1}^{\infty}\frac{(a\dot{z})^n}{n!} \\ &= \varepsilon f(z,\dot{z}).\end{aligned} \tag{9}$$

Introducing the following ansatz functions and abbreviations

$$z = A(t)\sin\theta(t) = AS \quad , \theta(t) = \omega_0 t + \psi \tag{10}$$

$$\dot{z} = A(t)\omega_0\cos\theta(t) = A\omega_0 C. \tag{11}$$

into eq. (9) yields the right-hand side

$$\varepsilon f(z,\dot{z}) = -2D\omega_0^2 AC + \frac{N\Delta\mu e^{-av_0}}{m}\left[\sum_{n=1}^{\infty}\frac{(aA\omega_0 C)^n}{n!}\right]. \tag{12}$$

Averaging gives the following amplitude equation

$$\dot{A} = \frac{1}{2\pi\omega_0}\int_{\theta=0}^{2\pi} f(z,\dot{z})\cos\theta d\theta \tag{13}$$

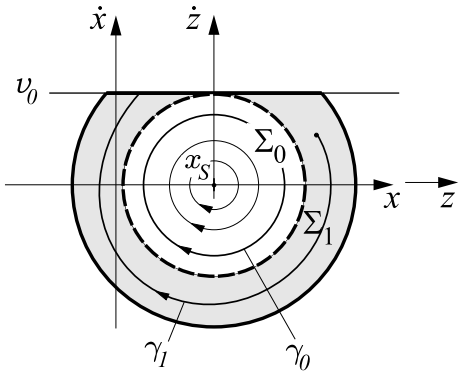

Figure 3. SET-UP OF THE PHASEPLANE. IN Σ_0 PERIODIC HARMONIC SOLUTIONS ARE POSSIBLE (e.g. γ_0), WHILE SOLUTIONS STARTING IN Σ_1 ARE IMMEDIATELY ATTRACTED BY THE STICK-SLIP LIMIT CYCLE (e.g. γ_1).

$$= -D\omega_0 A + \frac{N\Delta\mu e^{-av_0}}{2\pi m}\int_{\theta=0}^{2\pi}\sum_{n=1}^{\infty}\frac{a^n A^n \omega_0^{n-1} C^{n+1}}{n!}d\theta. \tag{14}$$

Due to the uniform convergence of the integrand, swapping integration and summation is allowed. Using the abbreviation

$$\int_{\theta=0}^{2\pi} a\, d\theta = \langle a \rangle \tag{15}$$

and considering that A is assumed to be constant during an averaging period $\theta = 0 \ldots 2\pi$, this leads to

$$\dot{A} = -D\omega_0 A + \frac{N\Delta\mu e^{-av_0}}{m}\sum_{n=1}^{\infty}\frac{a^n A^n \omega_0^{n-1}}{n!}\frac{\langle C^{n+1}\rangle}{2\pi}. \tag{16}$$

Now, half of the sum can be dropped since $\langle C^{2n+1}\rangle = 0 \;\; (n \in \mathbb{N})$. Resetting indices finally yields the following amplitude equation:

$$\dot{A} = -D\omega_0 A + \frac{N\Delta\mu e^{-av_0}}{m}\sum_{k=1}^{\infty}\frac{a^{2k-1}\omega_0^{2k-2}}{(2k-1)!}\frac{\langle C^{2k}\rangle}{2\pi}A^{2k-1}. \tag{17}$$

Since the right-hand side (12) does not contain any sine-terms, the phase keeps constantly zero:

$$\dot{\psi} = -\frac{1}{2\pi\omega_0 A}\int_{\theta=0}^{2\pi} f(z,\dot{z})\sin\theta d\theta = 0. \tag{18}$$

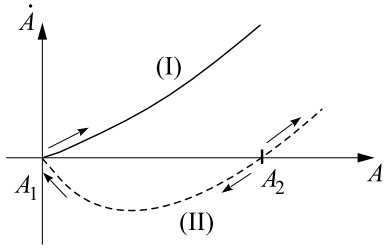

Figure 4. QUALITATIVE SKETCH OF THE AMPLITUDE GROWTH BEHAVIOR FOR CASES (I) AND (II).

Fixed points, limit cycles

To find fixed points or limit cycles, eq. (17) is investigated for solutions of stationary amplitudes with $\dot{A} = 0$. After that, the stability of these amplitudes is studied.

Regarding eq. (17) it is obvious that

$$A_1 = 0 \tag{19}$$

is always a possible stationary amplitude. Separating this solution from eq. (17) the following remains

$$\begin{aligned} 0 &= -D\omega_0 + \frac{N\Delta\mu e^{-av_0}}{m} \sum_{k=1}^{\infty} \frac{a^{2k-1}\omega_0^{2k-2}}{(2k-1)!} \frac{\langle C^{2k} \rangle}{2\pi} A^{2k-2} \qquad (20) \\ &= -D\omega_0 + \frac{N\Delta\mu e^{-av_0}}{m} \left[\frac{a}{2} + \sum_{k=2}^{\infty} \frac{a^{2k-1}\omega_0^{2k-2}}{(2k-1)!} \frac{\langle C^{2k} \rangle}{2\pi} A^{2k-2} \right], \end{aligned}$$

and hence

$$\frac{Dm\omega_0}{N\Delta\mu e^{-av_0}} - \frac{a}{2} = \sum_{k=2}^{\infty} \frac{a^{2k-1}\omega_0^{2k-2}}{(2k-1)!} \frac{\langle C^{2k} \rangle}{2\pi} A^{2k-2}. \tag{21}$$

Since all quantities are positive, eq. (21) can only hold for real, positive amplitudes A, if the difference of the left-hand side is positive. This yields a first equation for the existence of a limit cycle:

$$A_2 \in \mathbb{R}^+ \;\leftrightarrow\; \frac{Dm\omega_0}{N\Delta\mu e^{-av_0}} - \frac{a}{2} \overset{!}{>} 0. \tag{22}$$

In general, the differential equation (9) holds for $\dot{z} < v_0$, i.e. in the entire half plane of sliding below stiction line which is located at $\dot{z} = v_0$. But since periodic weakly-nonlinear oscillations are studied using a harmonic ansatz, the following considerations will only be valid within a phase-plane section containing solutions which are not immediately trapped by the stick-slip limit cycle. This section is denoted by Σ_0 (cf. fig. 3) and will be approximately of a circular shape for weak nonlinearities. By geometrical considerations, the radius of this approximate circular area will be $r = \frac{v_0}{\omega_0}$. With this, a limit-cycle in the sense of eq. (22) will only exist if the limit condition

$$A_2 \overset{!}{<} \frac{v_0}{\omega_0} \tag{23}$$

is fulfilled, as is e.g. for trajectory γ_0 in figure 3. Otherwise, the trajectory will soon end-up in the stick-slip limit cycle (e.g. γ_1 in figure 3).

Stability of fixed points and limit cycles

To study the stability of the stationary amplitudes given by (19) and (20), the first derivatives with respect to A are examined. Carrying out the derivations yields

$$\begin{aligned} \frac{d\dot{A}}{dA} &= -D\omega_0 + \frac{N\Delta\mu e^{-av_0}}{m} \sum_{k=1}^{\infty} \frac{a^{2k-1}\omega_0^{2k-2}}{(2k-1)!} \frac{\langle C^{2k} \rangle}{2\pi} (2k-1) A^{2k-2} \\ &= -D\omega_0 + \\ &\quad \frac{N\Delta\mu e^{-av_0}}{m} \left[\frac{a}{2} + \sum_{k=2}^{\infty} \frac{a^{2k-1}\omega_0^{2k-2}}{(2k-2)!} \frac{\langle C^{2k} \rangle}{2\pi} A^{2k-2} \right]. \qquad (24) \end{aligned}$$

Evaluation at the fixed point $A_1 = 0$ gives

$$\left. \frac{d\dot{A}}{dA} \right|_{A=A_1} = -D\omega_0 + \frac{N\Delta\mu e^{-av_0}}{m} \frac{a}{2}. \tag{25}$$

The fact that (24) reduces so dramatically corresponds to the theorem of Hopf and Andronov [5]. Depending on the parameters of the system, two cases can be outlined:

(I) $\left. \frac{d\dot{A}}{dA} \right|_{A=A_1} > 0$: the steady-state fixed point is unstable. Simultaneously condition (22) assuring the existence of the cycle is not fulfilled – hence there is only an *unstable fixed-point*. Figure 5 outlines this behavior qualitatively.

(II) $\left. \frac{d\dot{A}}{dA} \right|_{A=A_1} < 0$: the steady-state fixed point is stable and at the same time, condition (22) is fulfilled. Hence, there is an unstable limit cycle of amplitude A_2 coexisting to the stable fixed-point. The instability of limit-cycle can easily be seen from fig. 4, since small perturbations will be amplified. Hence there are a *stable fixed-point* and an *unstable limit-cycle* (see fig. 6). The amplitude A_2 of the unstable limit-cycle has to fulfill the limit condition (23) to avoid being swallowed by the stick-slip limit cycle.

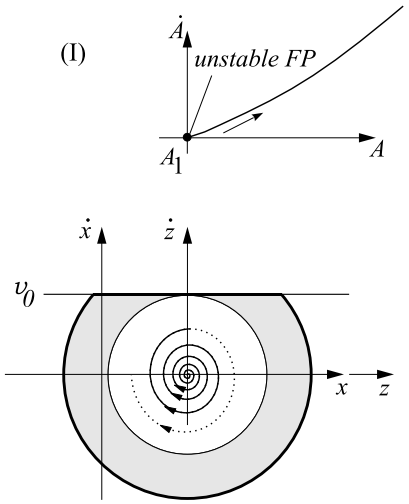

Figure 5. AMPLITUDE GROWTH AND PHASE PLOT. CASE (I): UNSTABLE FIXED POINT .

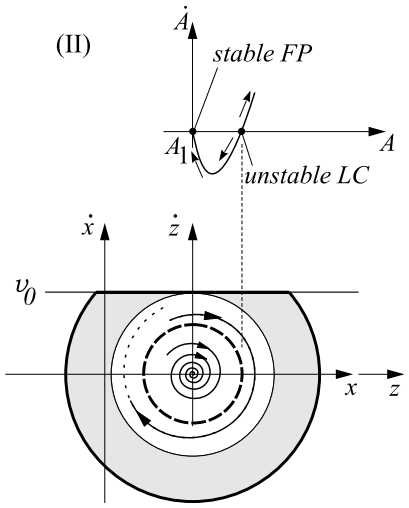

Figure 6. AMPLITUDE GROWTH AND PHASE PLOT. CASE (II): STABLE FIXED POINT AND UNSTABLE LIMIT CYCLE.

Figure 4 outlines qualitatively the growth behavior of the amplitdes for both cases. It is found, that the system can undergo a bifurcation, changing the phase plot from case (I) to (II) and vice versa, when parameters either of the oscillators or the friction curve are changed. The identified bifurcation behavior (i.e. unstable fixed-point ↔ stable fixed-point + unstable limit cycle) is referred to as *subcritical HOPF-Bifurcation*, cf. figures 5, 6.

SLIDING BIFURCATIONS – APPROXIMATE ANALYTICAL EVALUATION AND APPLICATION TO A DISC-BRAKE MODEL

Despite their exactness, the infinite sums involved in the amplitude equation (17) are not very comfortably to handle and only hardly allow insight in the behavior of the solution $z(t) = A\cos\theta$. To allow further analytical studies, the sum (17) is truncated after the cubic terms, i.e. dropping indices $k \geq 3$. This yields

$$\dot{A} = A\left[-D\omega_0 + \frac{N\Delta\mu e^{-av_0}}{m}\left(\frac{a}{2} + \frac{a^3\omega_0^2}{16}A^2 + O(A^4)\right)\right]. \quad (26)$$

Again, the fixed point

$$A_1^{(3)} = 0 \quad (27)$$

is obvious. Bracketed superscripts denote the truncation order. The second possible stationary amplitude is then found by simple calculus as

$$A_2^{(3)} = \frac{4}{a\omega_0}\sqrt{\frac{D\omega_0 m}{aN\Delta\mu e^{-av0}} - \frac{1}{2}} \quad . \quad (28)$$

This equation will only yield real amplitudes, if the radicand is positive or zero, what is equivalent to condition (22): if the radicand is negative an unstable fixed-point governs the sliding behavior – case (I) – while for a positive radicand, a stable fixed-point and an unstable limit-cycle can be observed – case (II). Between these two cases, the system undergoes the subcritical HOPF-Bifurcation when passing the borderline

$$0 = \frac{D\omega_0 m}{aN\Delta\mu e^{-av_0}} - \frac{1}{2}. \quad (29)$$

Although derived by a truncation of eq. (17), this equation is equivalent to eq. (22), which was derived from the averaged solution by exact analysis. Interestingly there is no loss of accuracy in the bifurcation border description due to the truncation. This is reasonable since at the bifurcation itself the amplitudes vanish and therefore the truncation has no further influence.

In addition, the amplitude of the unstable limit-cycle has to fulfill the approximate limit condition (23) to avoid entering the bassin Σ_1 and being attracted by the stick-slip limit-cycle.

Figure 7 shows the bifurcation behavior – and therefore the stability properties – of the disc-brake model described by the parameters given in Appendix A. While the black line denotes the HOPF-bifurcation, the grey line is given by the approximate limit condition (23), which counts for the fact that periodic harmonic

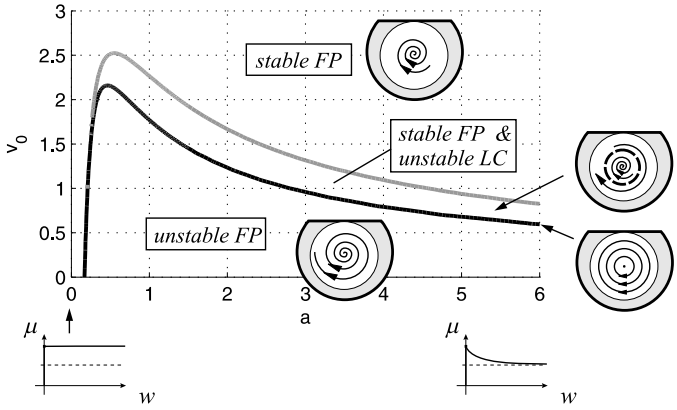

Figure 7. PATTERN PHASEPLOTS, BIFURCATION BORDER (BLACK LINE) AND APPROXIMATE EXISTENCE LIMIT OF THE UNSTABLE LIMIT CYCLE (GREY LINE) FOR A DISC BRAKE MODELL (cf. APPENDIX A).

solutions may only exist in the phase plane section Σ_0 (cf. fig. 3). It is emphasized that this grey line is only an approximation of condition (23) since it was derived by a truncation of (17) and the amplitudes do not vanish as they do at the black bifurcation line.

The qualitative behavior can be outlined as follows:

1. when passing the thick black line in direction of increasing belt velocity v_0, the unstable fixed-point turns stable and an unstable limit-cycle of amplitude A_2 (cf. eq. (28)) is born. Since it can only be observed unless its amplitude doesn't violate the limit condition (28), it vanishes when trespassing the thick grey line given by this condition.
2. when changing parameters in direction of the slope parameter a, for small values of a both borderlines can be passed simultaneously, i.e. the systems phase-flow changes almost instantaneously from an unstable to a stable fixed-point without exhibiting the limit-cycle. Surprisingly it is possible, that further increasing the slope parameter a can restabilize the system!

Figures 8, 9 and 10 show the the influence the damping D, the natural frequency $\omega_0 = \sqrt{\frac{c}{m}}$, which is varied by doubling and halving the stiffness of the system, and of the contact normal force N on the bifurcation behavior. It is found that higher damping, stiffness or lower contact normal force increase the parameter domain of the stable steady-state. But in all cases, low velocities v_0 stay critical in a parameter domain for a beyond a certain threshold. Even a damping of $D = 1$, which is a quite high value for real steel brake system, can't stabilize the steady-state.

In terms of the disc-brake model, consider that the ordinate v_0 denotes the surface velocity of the disc at the contact radius.

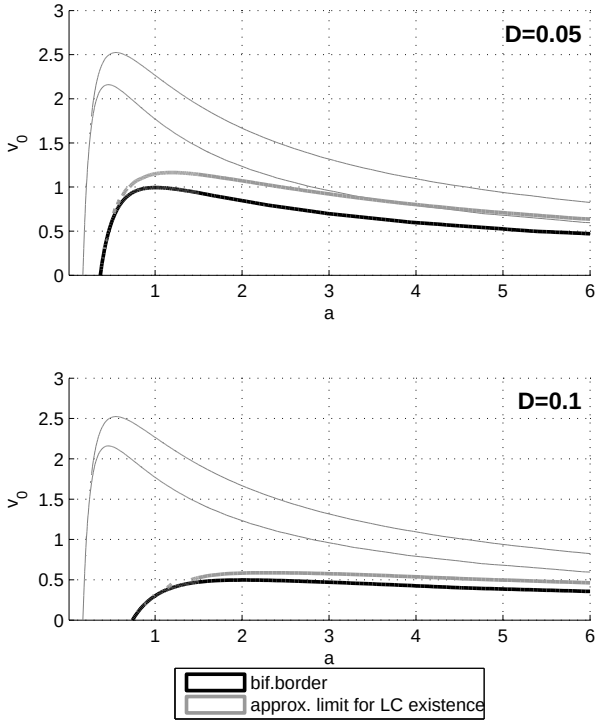

Figure 8. INFLUENCE OF THE DAMPING D ON THE BIFURCATION BORDER.
THIN LINES: $D_0 = 0.023$, BASIC CONFIGURATION (APPENDIX A)
UPPER: $D = 0.05$ – BOTTOM: $D = 0.1$.

The speed v_C of the car is given by

$$v_C = \frac{r_W}{r} v_0, \tag{30}$$

with r_W denoting the radius of the wheel and r being the distance from the axes to the contact point of the pad.

NUMERICAL SIMULATION OF A DISC BRAKE MODEL

Equation (1) is a typical example of a system exhibiting friction-induced vibrations and is therefore often chosen as a first model to study vibrations in disc-brakes. To evaluate the analytical results obtained above, also numerical simulations are done for these parameter sets. These simulations are carried out using the implicit variable time-step Runge-Kutta-Fehlberg scheme of order 2(3) provided by MATLAB (ODE23). In order to account for the unsteadiness of the general equation of motion (1), the event location function of MATLAB was used to switch between the particular differential equations.

In general, a direct simulation of unstable limit cycles is not possible. To deal with this, the fact was used, that unstable limit cycles are the repelling separatrix of two attractors and that this

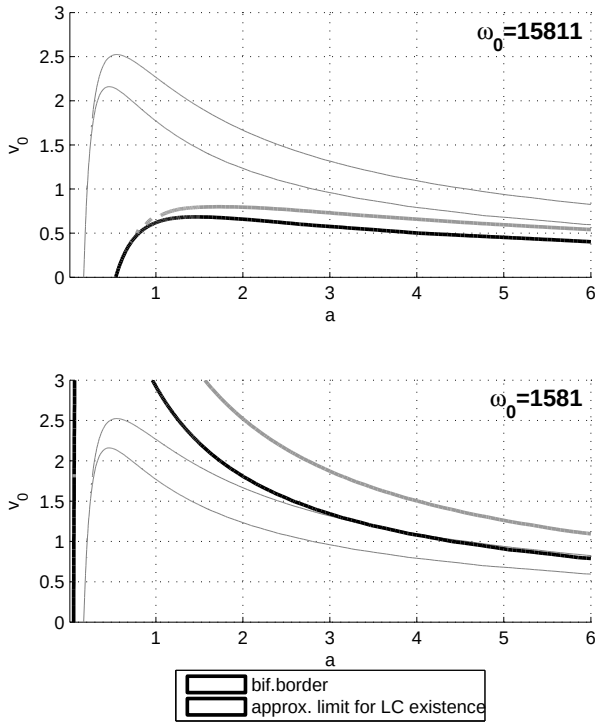

Figure 9. INFLUENCE OF THE NATURAL FREQUENCY ω_0 ON THE BIFURCATION BORDER.
THIN LINES: $\omega_0 = 5000\frac{\text{rad}}{\text{s}}$, BASIC CONFIGURATION (APPENDIX A)
UPPER: $\omega_0 = 15810\frac{\text{rad}}{\text{s}}$ (twice the stiffness)
BOTTOM: $\omega_0 = 1581\frac{\text{rad}}{\text{s}}$ (half the stiffness).

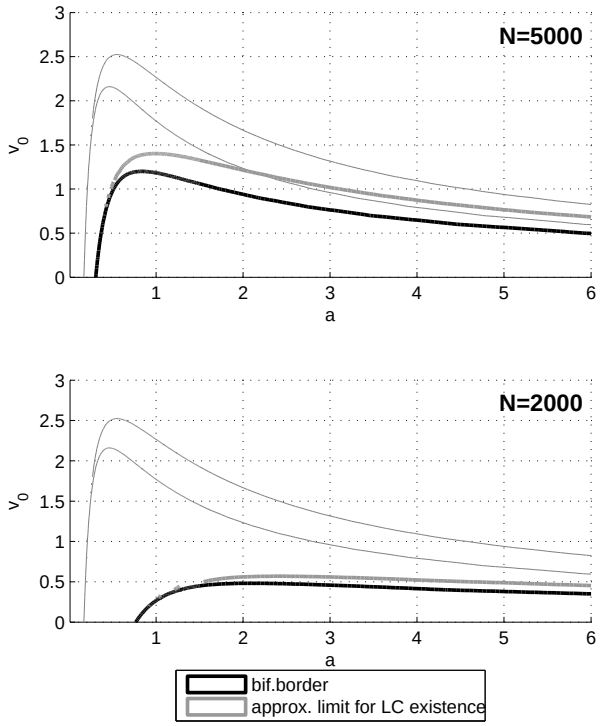

Figure 10. INFLUENCE OF THE CONTACT NORMAL FORCE N ON THE BIFURCATION BORDER.
THIN LINES: $N = 9000$N, BASIC CONFIGURATION (APPENDIX A)
UPPER: $N = 5000$N
BOTTOM: $N = 2000$N.

behavior is inverted when time is inverted. For this, the unstable limit cycles were obtained by inversion of time.

Figure 11 outlines the bifurcation borders for typical parameters for disc brake models, given in Appendix A, and shows the parameter combinations P1. . . P5 (see Appendix B) for which numerical simulations are carried out.

A comparison of the simulation results of the parameter sets P1, P2 and P3 displays how the topography of the phase-plane changes from the unstable fixed-point (P1, figure 12) to the twofold setup exhibiting a stable fixed-point and an unstable limit cycle (P2, figure 13) and finally to the stable fixed-point for set P3 (figure 14).

Figure 13 reveals an interesting aspect of the stability of the systems steady state: although there is a stable steady state in the sense of the classical stability analysis via eigenvalues (7), in a practical sense the system will probably be unstable since the bassin of attraction of the stable fixed-point, enclosed by the unstable limit cycle, is only very small. Even small (finite) perturbations of the steady state will be sufficient to let the system trespass the unstable limit cycle, leading it to the bassin of attraction of the stick-slip limit cycle. This example shows that

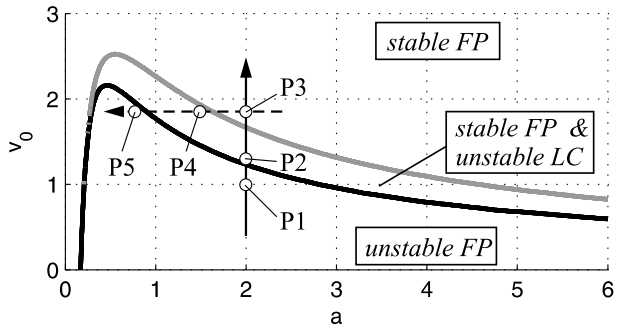

Figure 11. COMBINATIONS OF SIMULATION PARAMETERS (a, v_0) WITH THE SLOPE a OF THE FRICTION CHARACTERISTIC, AND THE SPEED v_0 OF BELT.

significant effects may stay undiscovered if only the eigenvalues of the linearized equation at the steady-state are examined.

Furthermore, looking at the systems behavior when parameters are changed to parameter set P4 and P5 reveals, that a reduction of the slope parameter a doesn't always cause a stabilization of the system. In contrast, changing from P3 (fig.14) over

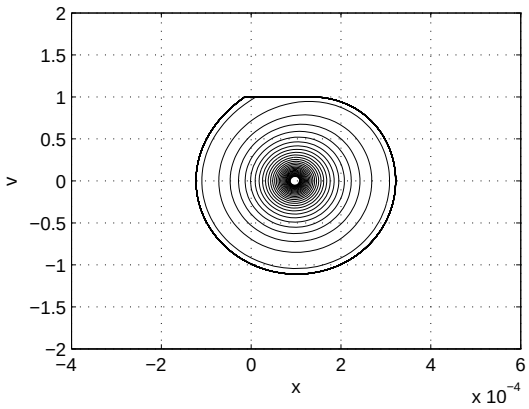

Figure 12. SIMULATED PHASE PLOT FOR PARAMETER SET P1: UNSTABLE FIXED POINT

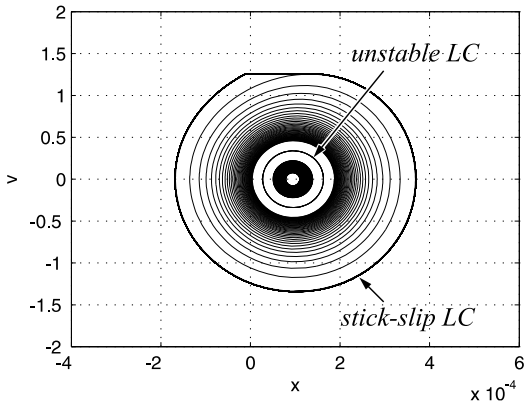

Figure 13. SIMULATED PHASE PLOT FOR PARAMETER SET P2: STABLE FIXED POINT & UNSTABLE LIMIT CYCLE.

P4 (fig.15) to set P5 (fig.16) leads to a destabilization of the the steady state – although the slope parameter a is reduced!

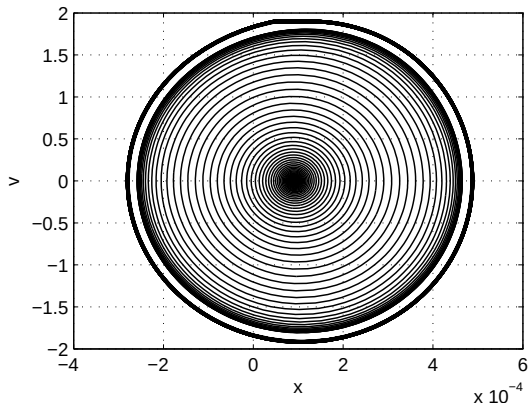

Figure 14. SIMULATED PHASE PLOT FOR PARAMETER SET P3: STABLE FIXED POINT & STABLE LIMIT CYLCE (ALMOST AT MAXIMUM AMPLITUDE).

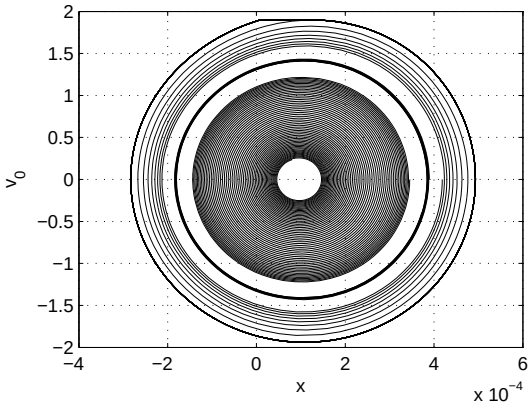

Figure 15. SIMULATED PHASE PLOT FOR PARAMETER SET P4: STABLE FIXED POINT & UNSTABLE LIMIT CYCLE.

CONCLUSION

Commonly, the stability of the classical friction oscillator is studied by linearization and examination of the eigenvalues. This article revises the stability in the vicinity of the sliding steady state for exponential-like friction characteristics, which are widely used in friction modelling. By means of a averaging method it is found that the transition behavior between stable and unstable states of sliding motion is more complex than suggested by the classical stability analysis. If sliding without reaching the stick-slip limit cycle, the topology of the phase plane is given by two possibilities: either the steady-state fixed point is unstable or it is stable and coexists with a surrounding unstable limit cycle. Interestingly, the bifurcation border coincidents with the stability border derived by eigenvalue analysis. The crux of the matter is, that the eigenvalue analysis only can judge the local behavior at the steady state while it does not indicate, that the bassin of attraction of the steady-state is limited to the inside of the unstable limit cycle. For that reason, besides the unstable domain there is also a region, where the steady-state itself is stable, but small perturbations may be sufficient for destabilization.

To demonstrate the effect, a disc-brake model is discussed. It is found that low disc speeds v_0 are extremely critical for a broad range of parameters. Surprisingly, even relative strong damping of $D = 0.1$ does not improve the situation significantly. Furthermore, it is found that e.g. for a relatively soft brake system, the motion can be stabilized by increasing the slope parameter a, which means increasing the declination of the friction characteristic.

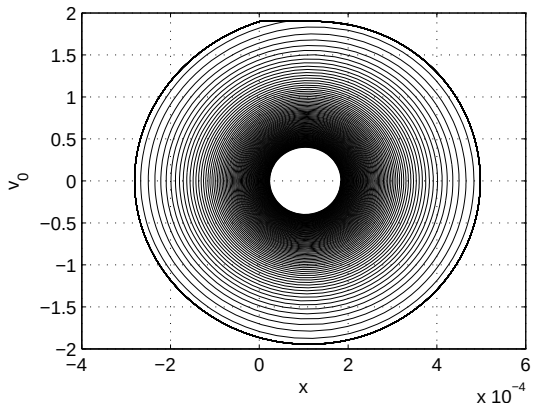

Figure 16. SIMULATED PHASE PLOT FOR PARAMETER SET P5: UNSTABLE FIXED POINT.

REFERENCES

[1] Kauderer, H., 1958. *Nichtlineare Mechanik*. Springer-Verlag, Berlin/G.

[2] Hagedorn, P., 1988. *Non-linear Oscillations*. Clarendon Press, Oxford.

[3] Magnus, K. ; Popp, K., 2002. *Schwingungen*. Teubner Verlag, Stuttgart.

[4] RA Ibrahim, E. R. "Friction-induced vibration, part i.". Applied Mechanics Reviews, **47** (7).

[5] J. Guckenheimer, P. H., 1983. *Nonlinear oscillations, dynamical systems, and bifurcations of vector fields*. Springer-Verlag, New York.

[6] U. von Wagner, T. Jearsiripongkul, e. "Brake squeal: modelling and experiments". VDI Bericht (1749).

[7] Schmalfuss, C. "Theoretische und experimentelle untersuchung von scheibenbremsen". VDI Fortschrittbericht (12) (494).

Appendix A: basic parameter configuration for the examined brake system

System:

m	=	1kg	moving parts of brake pads and saddle
ω_0	=	$5000\frac{\text{rad}}{s}$	natural frequency
D	=	0.023	dimensionless damping measure

Friction:

F_B	=	9kN	normal force on pad
μ_∞	=	0.25	sliding friction coefficient for $v_{rel} \to \infty$
$\Delta\mu$	=	0.15	$\Delta\mu$ at $v_{rel} = 0$ (cf.2)

Parameters were chosen according to [6], [7].

Appendix B: parameter combinations for numerical simulation

P1: $a = 2\,\text{s/m}, v_0 = 1\,\text{m/s}$ — P2: $a = 2\,\text{s/m}, v_0 = 1.2\,\text{m/s}$
P3: $a = 2\,\text{s/m}, v_0 = 1.9\,\text{m/s}$ — P4: $a = 1.55\,\text{s/m}, v_0 = 1.9\,\text{m/s}$
P5: $a = 0.75\,\text{s/m}, v_0 = 1.9\,\text{m/s}$